



Magnetic phase diagram of MnGa_2Se_4 compound

R. Cadenas^{a,b,*}, M. Quintero^a, E. Quintero^a, R. Tovar^a, M. Morocoima^a,
J. González^a, J. Ruiz^a, J.M. Broto^c, H. Rakoto^c, J.C. Woolley^d, G. Lamarche^d

^aDepartamento de Física, Facultad de Ciencias, Centro de Estudio de Semiconductores, Universidad de los Andes, Mérida, Venezuela

^bDepartamento de Física, Facultad de Ciencias, Universidad del Zulia, Maracaibo, Venezuela

^cUniversité Toulouse III. LNCMP 143 avenue de Rangueil, 31432 Toulouse Cedex, France

^dOttawa-Carleton Institute for Physics, University of Ottawa, Canada K1N 6N5

Abstract

The magnetic phase diagram of MnGa_2Se_4 was obtained by means of low magnetic field susceptibility in the temperature range from 2 to 300 K and high magnetic field magnetization measurements at several temperatures between 2 and 150 K, by using a MPMS-5 magnetometer and pulsed magnetic fields method, respectively. The obtained results show that the phase diagram is consistent with the uniaxial antiferromagnetic material when the field is applied parallel to the easy axis.

© 2004 Elsevier B.V. All rights reserved.

PACS: 75.50.Pp; 75.50.Ee; 75.30.Cr; 75.30.Kz

Keywords: Semimagnetic semiconductors; Antiferromagnets; Magnetic susceptibility; Magnetic phase diagram; High magnetic fields; Pulsed magnetic fields; Spin–flop transition

The MnGa_2Se_4 semimagnetic semiconductor belongs to the class of defective semiconductors with general formula $\text{II-III}_2\text{-}\square\text{-VI}_4$, where the symbol “ \square ” stays for one vacancy. The MnGa_2Se_4 compound is a direct energy gap material crystallizing in the tetragonal structure with space group $I\bar{4}$ [1]. The cations are ordered on sites with Se environment.

In this paper we report the magnetic susceptibility measurements and the magnetic behavior at high magnetic fields of a polycrystalline sample of

MnGa_2Se_4 compound prepared by the melt and anneal technique [2].

The LMF measurements, $B \leq 5$ T, were performed with the MPMS-5 DC SQUID magnetometer (Merida) and the zero-field-cooled (ZFC) and field-cooled (FC) data was obtained in the temperature range from 2 to 300 K. The details of the ZFC–FC procedure was the following: the temperature of the sample was reduced in zero field (ZFC) down to about 2 K; at this temperature a DC field was applied and the magnetization was measured with the temperature rising to about 300 K. After that the sample was cooled again keeping the field constant (FC) and the data was obtained as a function of decreasing T . On the other hand, data at higher fields, up to 35 T, were

*Corresponding author. Departamento de Física, Facultad de Ciencias, Universidad del Zulia, Aptdo. 526, Maracaibo, Venezuela.

E-mail address: rcadenas@luz.ve (R. Cadenas).

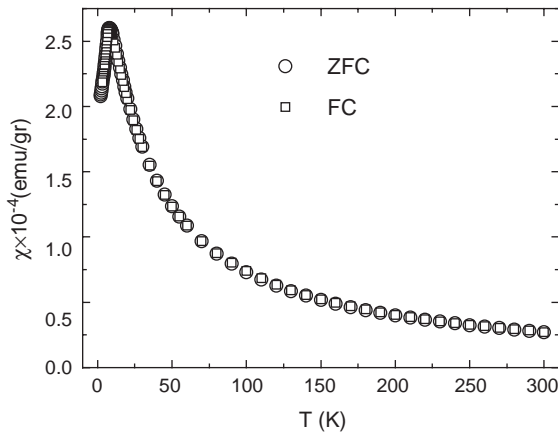


Fig. 1. ZFC and FC susceptibility χ vs. T curve for the MnGa_2Se_4 compound measured at 5×10^{-3} T.

obtained using the Laboratory's pulsed magnetic fields facility in Toulouse.

Fig. 1 shows the susceptibility χ vs. T of the MnGa_2Se_4 compound measured at $B = 5 \times 10^{-3}$ T. No temperature hysteresis was observed between the ZFC and FC susceptibility measurements and the overall behavior agrees with those of an AFM.

The Néel temperature, $T_N = 8.2$ K, was obtained from the cusp of the χ vs. T curve and it is seen from the $1/\chi$ vs. T curve (not shown) that this curve is linear down to, approximately, the Néel temperature. The extrapolation of the $1/\chi$ vs. T curve allows to obtain the Curie–Weiss temperature $\theta = -22$ K.

Fig. 2 shows the M vs. B curves obtained at fixed temperatures between 2 and 150 K for the MnGa_2Se_4 compound by using the PMF method. As can be seen, there are hysteresis effects that may be due to the polycrystalline character of the sample [3]. However, it is noted that the hysteresis is related to the antiferromagnetic (AF) transition because the hysteresis is more evident when the temperature is close to the Néel temperature. This effect seems to be the expected when the Spin-Flop (SF) transition is going to occur [4,5]. Then, assuming that the AF transition occurs at 8.2 K we expect that a SF transition would appear below 8.2 K.

Most theoretical treatments of phase transitions in AFM consider the case of uniaxial AFM of the

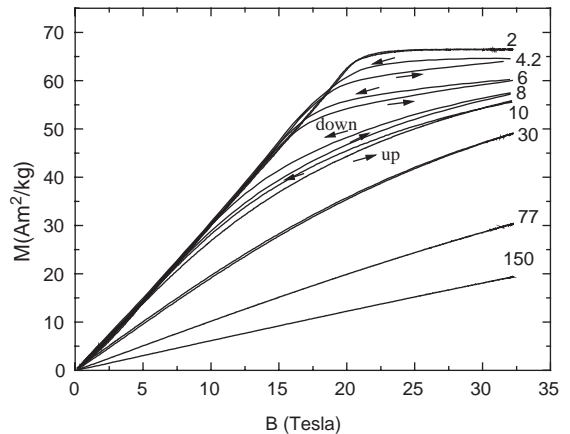


Fig. 2. M vs. B curves for the MnGa_2Se_4 measured at several temperatures. The arrows along the curves indicate the directions of the field sweep.

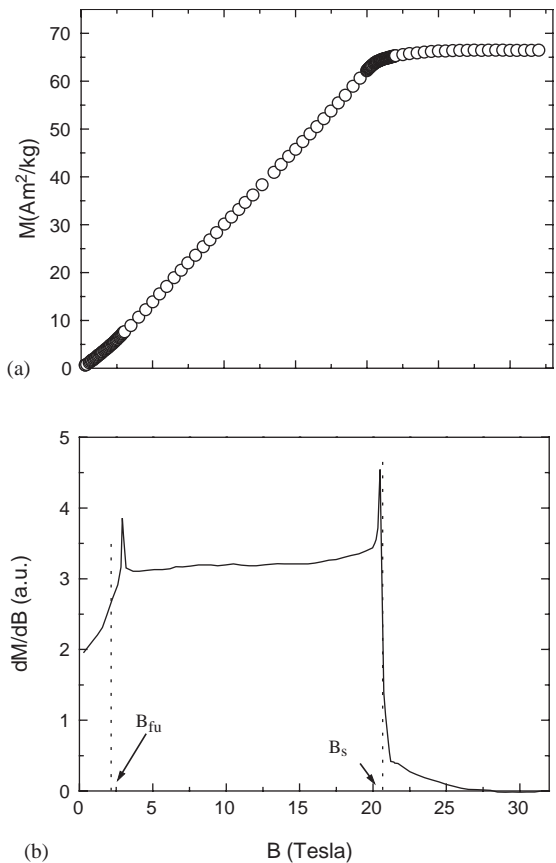


Fig. 3. (a) M vs. B curve for the MnGa_2Se_4 at 2 K measured with increasing field. (b) Differential susceptibility, dM/dB , vs. B obtained numerically from the results in (a).

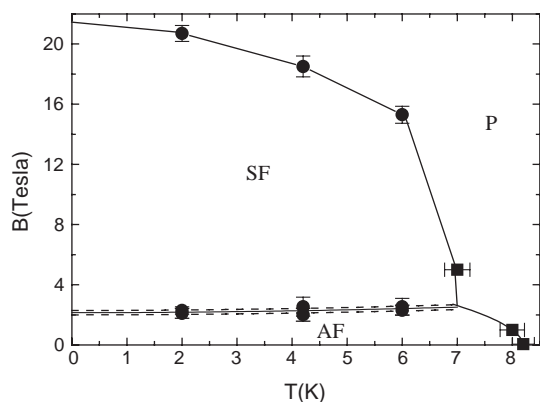


Fig. 4. Magnetic phase diagram, $B(T)$, for the MnGa_2Se_4 . The “●” points are obtained from the M vs. B curves and the “■” points from the susceptibility data. AF, SF and P stay for the antiferromagnetic, spin-flop and paramagnetic phase, respectively.

easy-axis type. These theoretical analysis (e.g. [6,7]) show that for an AFM three phases can occur in the magnetic phase diagram; the paramagnetic (P), the AF and the SF phases. Lines of interest in the diagram are the transitions between the phases, i.e. AF-SF (B_f), the spin-flop field, and AF-P, and SF-P (B_s), the saturation field.

The phase transitions can be determined better if dM/dB is considered rather than M as illustrated in Fig. 3 where dM/dB is plotted against the increasing field B for the magnetization curve measured at 2 K. The values of the critical SF fields were estimated from the inflexion points at the left side of the first peak in the dM/dB vs. B curves. Because of the hysteresis there will be two different values of the critical SF field for increasing (B_{fu}) and for decreasing fields (B_{fd}).

The sharp drop at higher fields located the transition to the P state at $B=B_s$. The present analysis was carried out for all the M vs. B curves for temperatures below T_N .

Fig. 4 shows the PMF results (vertical error lines) together with the LMF ones (horizontal error lines) and represents the proposed magnetic phase diagram, $B(T)$, for the MnGa_2Se_4 compound. A complete quantitative analysis for the $B(T)$ phase diagram will be given in a further work.

Acknowledgements

This work was supported by the PCP (France)-CONICIT (Venezuela) Nanomaterials and CDCH-ULA. RC wishes to thank the Embassy of France in Venezuela, and JG thanks the Alfa-Program (Project number II0147FI), for financial support.

References

- [1] M. Quintero, M. Morocoima, E. Guerrero, J. Ruiz, Phys. Stat. Sol. (a) 146 (1994) 587.
- [2] M. Quintero, A. Barreto, P. Grima, R. Tovar, G. Sánchez, J. Ruiz, J.C. Woolley, G. Lamarche, A.-M. Lamarche, Mater. Res. Bull. 34 (1999) 2263.
- [3] M. Hase, N. Kooide, K. Manabe, Y. Sasago, K. Uchinokura, A. Sawa. Physica B 215 (1995) 164.
- [4] I.S. Jacobs, J. Appl. Phys. 32 (1961) 61S.
- [5] K.W. Blazey, K.A. Muller, M. Ondris, H. Rohrer, Phys. Rev. Lett. 24 (1970) 105.
- [6] Y. Shapira, S. Foner, Phys. Rev. B 1 (1970) 3083.
- [7] K.W. Blazey, H. Rohrer, R. Webster, Phys. Rev. B 4 (1971) 2287.